JOURNAL OF CONTENT VALIDATION 2026, VOL 2, ISSUE 2, PAGES 136-147
ISSN: 3093-8317, https://doi.org/10.67211, www.cvsgm.org

Design and Development of Deep Learning based Technique for Image Denoising

Pranita Jadhav[1*], Meenakshi Pawar[2], Swati Pawar[3]

[1 2 3] *SVERI's COEP, Solapur University, India*

**Corresponding Author Email: - akshatasjadhav1996@gmail.com*

Received: 10 March 2025 • Accepted: 19 April 2026 • Published: 15 June 2026

Abstract

The viability of GANs in picture denoising is wonderful, yet the test stays in adjusting commotion evacuation while safeguarding picture subtleties. Here, we present a changed Progressive Generative Ill-disposed Organization (Howdy GAN). The principal generator holds high-recurrence components, for example, edges and surfaces, the second recovers low-recurrence attributes and the third upgrades recreation execution. We changed the Leftover Thick Block (RDB) by adding a ReLU layer and a convolution to diminish the possibility evaporating angles, bringing about quicker learning and further developed execution. By and large, the proposed Greetings GAN model beats the impediments of existing picture denoising calculations and offers prevalent execution in safeguarding picture subtleties while eliminating clamor.

Keywords: *Convolutional and de-convolutional neural networks, deep learning*

INTRODUCTION

Computerized pictures assume a vital part in numerous parts of our day to day existence, such as satellite television, clever traffic observing, signature confirmation and penmanship acknowledgment on checks. Anyway they assume indispensable part at logical and mechanical fields, for example, geographic data channels and other data on pictures. A few elements are unavoidably impacted by commotion during the time spent procurement, pressure and transmission, bringing about twisting and loss of picture information [19]. Picture de-noising has impacted practically all specialized fields and assumes a significant part in many fields like transmission and coding, minute imaging, lawful sciences, picture remaking, visual following, picture enlistment, picture division and picture plan. For vigorous execution it is fundamental for protect the substance of the first picture [10]. Picture de-noising methods have been generally considered and created as of late to address the difficulties of sound decrease in pictures. Numerous calculations and techniques have been proposed to accomplish improved brings about picture de-noising. A few famous techniques incorporate separating based approaches, wavelet-based approaches, and

profound learning-based approaches [18]. Sifting based approaches plan to diminish commotion by applying channels to the picture. These channels can be planned in light of different measures like mean separating, middle sifting, and bilateral filtering. Wavelet-based approaches use wavelet change to decay the picture into various recurrence parts and afterward perform denoising on every part independently. Profound learning-based approaches utilize profound brain organizations to become familiar with the planning among loud and clean pictures. They have shown great outcomes in different undertakings, including picture denoising. One of the difficulties in picture denoising is to adjust sound decrease and picture detail protection. In the event that the denoising calculation eliminates a lot of commotion, it might likewise.

Eliminate a few significant subtleties and highlights of the picture. Then again, on the off chance that the calculation is excessively moderate, it may not eliminate sufficient commotion, bringing about a loud picture. Consequently, finding a decent harmony between sound decrease and picture detail conservation is pivotal for accomplishing top notch denoised pictures. All in all, picture denoising is a significant issue in different fields of examination and has been broadly concentrated on in late years[8]. The proposed increase calculation prepares numerous generators simultaneously,and every generator figures out how to denoise an alternate subset of the picture information. This permits every generator to spend significant time in eliminating a particular kind of clamor, consequently keeping away from mode breakdown and further developing the generally denoising execution. At long last, our third system is to present an original perceptual misfortune capability, which considers the significant level elements of the picture, notwithstanding the customary pixel-wise MSE misfortune capability. This assists with protecting the picture content and surface subtleties, while likewise lessening the relics and working on the generally perceptual nature of the denoised images.In synopsis, our proposed denoising strategy joins an effective ill-disposed misfortune capability, another expansion calculation for preparing various generators, and an original perceptual misfortune capability, to accomplish both high-precision and great discernment in denoising. Exploratory outcomes show that our strategy beats existing cutting edge techniques as far as both PSNR and perceptual quality, while likewise keeping away from the issue of mode breakdown. The changed B-DenseUNet(Boosted DenseUNet) design for proposed Hello GAN generators joins the upsides of Lingering Thick Blocks (RDB) and UNets to permit most extreme data move through all convolutional layers in the organization. This design improves the viability of proposed. Greetings GAN generators, which can be proficiently prepared by joining every one of the upsides of its generators while keeping away from their burdens. By using refitted B-DenseUNet, the altered HI-GAN can achieve state-of-the-art results in terms of both PSNR and visual quality, and can effectively remove noise from images while preserving image details. Overall, the proposed HI-GAN with adjusted B-DenseUNet architecture shows promising results for image denoising tasks and can be applied to a great many reasonable applications in different fields (Hossen et al., 2026).

The main objectives of this study are as follows: Examine existing methods and find out the limitations of image denoising. Design and develop a novel neural convolutional network for image noise reduction. Test various performance indicators of the proposed system, such as accuracy, precision, PSNR (peak signal-to-noise ratio) and so on. Compute the first picture by eradicating commotion from a form of the picture that has clamor in it image processing, with numerous studies focusing on improving image quality through advanced machine learning and deep learning techniques. Early studies demonstrated that multi-layer perceptrons (MLPs) trained on image patches could directly learn the mapping between noisy and clean images, achieving performance comparable to state-of-the-art denoising methods. Other researchers introduced frameworks that combined sparse coding and deep neural networks for blind image inpainting and denoising, enabling image colorization and denoising within a unified architecture. Further advancements were made through adaptive multi-column stacked sparse denoising autoencoders, which effectively handled various noise types without requiring prior knowledge of the noise distribution during testing (Alam et al., 2025).

Several studies have emphasized the role of large-scale datasets and convolutional neural networks (CNNs) in improving denoising performance. Research has shown that training on extensive image datasets can outperform many traditional denoising approaches. In medical imaging applications, comparative analyses of different filtering techniques for MRI image denoising revealed that median filtering often produces favorable results. Lightweight CNN-based architectures have also been proposed for image denoising and enhancement, achieving improved performance through effective data preprocessing and augmentation techniques. Furthermore, residual learning-based deep convolutional neural networks have demonstrated the ability to effectively separate noise from noisy

observations, thereby improving denoising accuracy (Mohd Pauzi & Shahadat Hossen, 2025).

Deep learning-based image denoising methods have continued to evolve with increasingly sophisticated architectures. CNN-based denoising approaches have proven effective in removing Gaussian noise while improving the efficiency of conventional filtering methods. These approaches have also been extended to address salt-and-pepper noise. Generative adversarial network-based frameworks have further enhanced denoising performance by employing adversarial loss functions to reduce statistical noise in digital radiological images while producing visually appealing results. Flexible CNN models that incorporate noise-level maps into network training and design have also enabled discriminative denoising under varying noise conditions (Hossen et al., 2023).

Recent advancements have focused on improving network depth, adaptability, and self-supervised learning capabilities. Deep iterative down-up networks utilizing U-Net-based architectures have demonstrated strong performance in handling different levels of Gaussian noise through iterative down-sampling and up-sampling operations. Self-guided neural networks employing self-routing mechanisms have been proposed to progressively recover multi-scale contextual information during image restoration. In addition, self-supervised learning approaches have emerged as significant innovations, enabling CNN-based denoising using only noisy image data without requiring clean reference images. These methods have been successfully applied across various imaging domains, including photography, fluorescence microscopy, and cryo-electron microscopy (Rashed et al., 2025).

Several review and comparative studies have contributed to understanding the strengths and limitations of different denoising approaches. Comprehensive reviews have critically evaluated recent developments in image denoising techniques and highlighted their advantages and drawbacks. Comparative analyses of CNN-based denoising methods have shown superior performance over conventional techniques based on metrics such as Peak Signal-to-Noise Ratio (PSNR), Structural Similarity Index Measure (SSIM), and Mean Squared Error (MSE). Hybrid models integrating multidirectional Long Short-Term Memory (LSTM) networks with CNN architectures have further improved both objective and subjective image quality (Rahman et al., 2025).

Moreover, researchers have examined the effectiveness of CNN-based denoising frameworks that incorporate techniques such as Batch Normalization (BN), Rectified Linear Unit (ReLU) activation functions, and residual learning to enhance denoising performance. Comprehensive analyses of deep learning-based denoising methods have covered a wide range of noise models, network architectures, and application scenarios. More recently, physics-based noise generation and calibration models have been developed to address denoising challenges in extremely low-light environments. Overall, the existing literature demonstrates the growing effectiveness of deep learning approaches, particularly CNN-based models, in addressing complex image denoising challenges across diverse application domains. These advancements have significantly improved image restoration quality and continue to drive innovation in computer vision and image processing research.

A. Deep Neural Networks for Image Denoising

There have been a few endeavors to address the de-noising issue utilizing profound brain organizations. In Jain and Seung's work, they proposed the utilization of convolutional brain organizations (CNNs) for picture de-noising and asserted that CNNs have comparative or far better execution than MRF models in delivering. Among the previously mentioned profound brain network-based techniques, MLP and TNRD can accomplish promising execution and contend with BM3D.

B. Residual Learning

The residual learning technique for convolutional neural networks (CNNs) was originally proposed to address the problem of performance degradation, where the training accuracy decreases as the network depth increases. In residual networks, the model explicitly learns residual maps for some stacked layers, assuming that these residual maps are easier to learn than the original unreferenced maps. This strategy of learning residual maps has enabled the training of extremely deep CNNs with ease, leading to improved accuracy in image classification and object recognition.

C. GAN

In 2016, Goodfellow et al. proposed the generative adversarial network (GAN), which led to a lot of related research. Some researchers explored image style transfer, such as the Cycle GAN proposed by B. Bair et al., which they viewed as an image-to-image translation problem. Others, like Orest Kupyn et al., proposed Deblur GAN to remove blind motion [4]. Among these studies, one author designed a GAN-based deep residual network and proposed a loss function for network training. In their training results, the well-designed loss function not only improved the resolution of the image but also enhanced the content and color of the original image, preserving many details.

DATA SET

The implementation procedure involved using two datasets, namely SIDD [12] and FFHQ. The SIDD dataset consists of 320 natural images, while the FFHQ dataset has 52,000 high-quality PNG images with a resolution of 512×512, showing significant variance in age, race, and image background. Randomly cropped training patches of size 512×512 were obtained from randomly selected images in these datasets. Noise and ground truth patch pairs were generated by the noise model for synthesizing real noise. The PyTorch machine learning library was used for training the model. To test our methodology, we used an Nvidia GTX 1080 Ti graphics card. Assessment measures were also used to evaluate the performance of the model.

MODEL ARCHITECTURE

The proposed modified HI-GAN consists of Gb, Ga, Da discriminator [26], and Gc gain network. Gb and Ga are both image denoising DCNN generators. Additionally Ga and Da are trained together to enhance Ga's capacity for denoising and detail preservation in distorted images. Ga's advantage lies in its ability to address the issue of missing high frequency features like edges and textures by persistently engaging in recurrent zero-sum games with Da. Gb, on the other hand, is trained independently and is not in competition with any network. Gb's technique is to ignore the discriminator's influence on instability and concentrate solely on denoising. In general, Gb and Ga use distinct methods and criteria to assess the effectiveness of rebuilding, and neither is superior to the other. We proposed a modified residual dense block (RDB) in our regenerated HIGAN to fully utilize all hierarchical features from the original LR image. It is unreasonable for an extremely profound organization to remove the result of each convolutional layer in the LR space. Consequently, we present RDB as the structure module for current HIGAN. RDB comprises of thick associated layers and neighborhood include combination (LFF) with nearby lingering learning (LRL). Our RDB likewise upholds coterminous memory among RDBs. The result of one RDB has direct admittance to each layer of the following RDB, bringing about a coterminous state pass. Each convolutional layer in RDB approaches generally ensuing layers and gives data that should be protected. LFF extricates nearby thick elements by adaptively saving data and connecting the conditions of going before RDB and all first layers inside the ongoing RDB. Moreover, LFF considers a high development rate by balancing out the preparation of a more extensive organization. Subsequent to extricating staggered neighborhood thick elements, we conductThe proposed altered Hey GAN comprises of Gb, Ga, Da discriminator[26], and Gc gain organization. Gb and Ga are both picture denoising DCNN generators. Also, Ga and Da are prepared together to improve Ga's ability for denoising and detail safeguarding in twisted pictures. Ga's benefit lies in its capacity to resolve the issue of missing high recurrence highlights like edges and surfaces by steadily captivating in repetitive zero-su games with Da. Gb, then again, is prepared freely and isn't in rivalry with any organization. Gb's strategy is to disregard the discriminator's effect on insecurity and focus exclusively on denoising. As a rule, Gb and Ga utilize particular techniques and measures to survey the viability of revamping, nor is better than the other. We proposed a changed leftover thick block (RDB) in our recovered HIGAN to completely use all various leveled highlights from the first LR picture. It is illogical for a very deep network to extract the output of each convolutional layer in the LR space. Therefore, we introduce RDB as the building module for modern HIGAN. RDB consists of dense connected layers and local feature fusion (LFF) with local residual learning (LRL).

Our RDB also supports contiguous memory among RDBs. The output of one RDB has direct access to each layer of the next RDB, resulting in a contiguous state pass. Each convolutional layer in RDB has access to all subsequent layers and passes on information that needs to be preserved. LFF extracts local dense features by adaptively preserving information and concatenating the states of preceding RDB and all preceding layers within the current RDB. Additionally, LFF allows for a high growth rate by stabilizing the training of a wider network. After extracting multi-level local dense features, To further improve the information flow, we introduce local residual learning
(LRL) in the RDB, as there are several convolutional layers in one RDB. The final output of the -th RDB can be obtained by It should be noted that LRL can also further improve the network's representation ability, resulting in

better performance. Due to the dense connectivity and local residual learning, we refer to this block architecture as a Residual Dense Block (RDB).

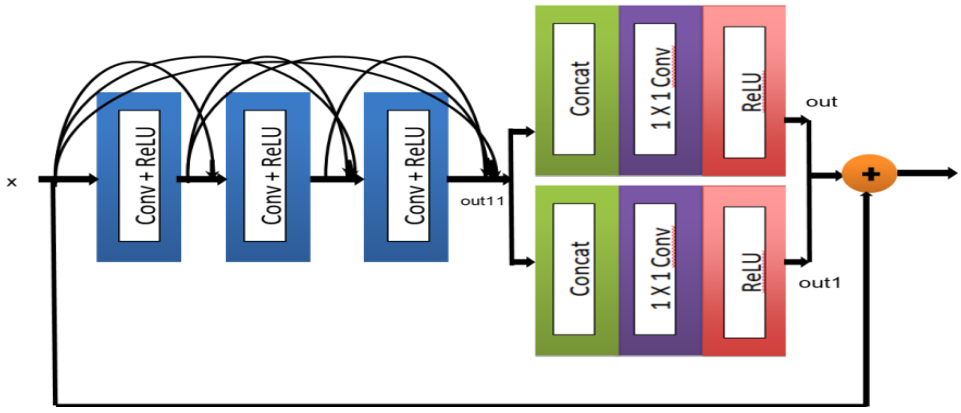

Figure 1. Refitted Residual Dense Block

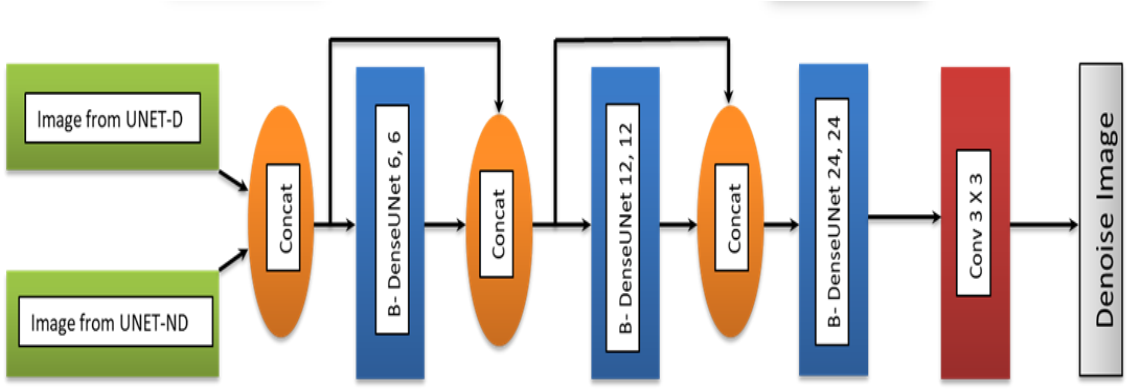

Figure 2. Block Diagram of modified Gc.

Figure 3. Block diagram of proposed B-DenseUNet used in the generators including Ga and Gb.

In this section, we will describe the implementation procedure and provide details about the experiments, including the datasets used and the evaluation metrics employed.

A. Testing Datasets

We utilized the DND [9], SIDD [12], and NAM [7] databases to compare the accuracy of the proposed method with its competitors. The DND dataset is designed to evaluate PSNR and SSIM on real-world photos, with competing methods evaluated through an online submission mechanism. It consists of 50 pairs of real noisy images and ground truth images. SIDD, on the other hand, evaluates the PSNR and SSIM of natural images taken by smartphone cameras, containing numerous pairs of photos taken in related scenes with various lighting setups. The performance ratings for the SIDD dataset are also based on an online submission method, like the DND dataset. Finally, we used 11 test images from the NAM dataset to assess and compare the reconstruction capabilities of different methods.

B. Evaluation metrics

1) Peak signal to noise ratio (PSNR)

The Peak Signal-to-Noise Ratio (PSNR) is a metric used to evaluate the visual quality of images by measuring the difference between corresponding pixels. It has been shown to be correlated with the average opinion scores provided by human experts. PSNR is essentially an MSE-based feature. The distortion level of an image after steganography is influenced by the size of the pixel values.

2) Structural similarity index (SSIM)

The SSIM metric evaluates the structural similarity, brightness, and contrast of images and can be used to assess the quality of steganographic images. As SSIM values increase, it indicates that the image before and after steganography are more similar in terms of structural content.

The equation provided is the formula for calculating the SSIM index between two images x and y. The symbols l(•), c(•), and s(•) represent luminance, contrast and structure, respectively. and are the pixel averages of image x and image y, respectively; and represent the standard deviations of image x and image y; denotes the covariance of image x and image y.

RESULTS

The de-noising results for the SIDD, DND, FFHQ, and NAM datasets are introduced in Table 1 and 2, including PSNR and SSIM scores. In the proposed HIGAN model, the changed Lingering Thick Block (RDB) has prompted an expansion in the PSNR and SSIM of pictures by a normal of 3.314 in PSNR and 0.1633 in SSIM. By accomplishing higher PSNR and SSIM, the point of our organization has been achieved. Tables 4 to 7 exhibit the subjective assessment of the contending calculations. The Hello GAN can catch perceptually high surfaces and significant subtleties, while the past technique produces more ancient rarities and clamor contrasted with the adjusted Greetings GAN.

Table 1. Result of SIDD and DND Dataset

Sr. No.	**SIDD**		**DND**	
	PSNR/SSIM by HIGAN	PSNR/SSIM by our model	PSNR/SSIM by HIGAN	PSNR/SSIM by our model
1	32.56/0.9527	35.93/0.971	27.5/0.5911	31.74/0.8966
2	32.95/0.9525	36.04/0.9704	27.05/0.5744	30.04/0.8532
3	27.11/0.9318	29.62/0.9298	27.09/0.549	30.7/0.8437
4	27.13/0.9308	29.67/0.9284	27.7/0.5673	30.48/0.8851
5	35.66/0.9352	38.36/0.9846	27.74/0.5396	30.35/0.9138
6	31.63/0.9154	36.04/0.9784	26.27/0.5861	32.36/0.8437
7	38.45/0.9552	41.17/0.9852	27.06/0.6359	30.16/0.9019
8	35.95/0.949	39.62/0.9794	27.31/0.6189	30.06/0.8868
9	40.27/0.9737	40.87/0.978	27.45/0.626	28.55/0.89
10	34.09/0.9531	36.78/0.9805	27.5/0.6876	28.53/0.8966
	33.58/0.9449	**36.41/0.96857**	27.267/0.597	**30.297/0.881**

Table 2. Result of FFHQ and NAM Dataset

Sr. No.	**FFHQ**		**NAM**	
	PSNR/SSIM by HIGAN	PSNR/SSIM by our model	PSNR/SSIM by HIGAN	PSNR/SSIM by our model
1	27.25/0.6226	31.64/0.8941	37.94/0.9559	40.79/0.9821
2	27.38/0.6375	31.97/0.9277	39.13/0.9418	42.62/0.9791
3	27.14/0.5935	32.05/0.8908	41.19/0.9537	43.9/0.9855

4	27/0.6052	32.66/0.9205	37.78/0.9276	40.04/0.964
5	26.62/0.6691	28.34/0.914	39.12/0.9486	43.3/0.9736
6	27.2/0.6194	31.31/0.9258	38.04/0.9107	40.97/0.9731
7	27.23/0.6097	30.65/0.9247	35.35/0.9026	38.57/0.9535
8	27.39/0.6289	32.7/0.9362	37.73/0.9438	38.61/0.9753
9	27.34/0.6106	32.62/0.9244	33.92/0.8583	39.35/0.9601
10	27.23/0.6295	30.46/0.924	33.65/0.8406	37.07/0.9516
	27.178/0.6226	**31.44/0.9182**	37.385/0.91836	**40.522/0.969**

Table 3. Comparison of HIGAN and Our Model

Dataset	**HIGAN**	**Our Model**
SIDD	33.58/0.9449	**36.41/0.96857**
DND	27.267/0.597	**30.297/0.881**
FFHQ	27.178/0.6226	**31.44/0.9182**
NAM	37.385/0.91836	**40.522/0.969**

Table 4. Result of SIDD Dataset

Noisy Image	HI-GAN Denoised Image	Denoised Image by Our Method	Clean Image
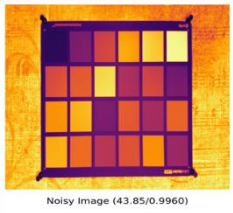 Noisy Image (43.85/0.9960)	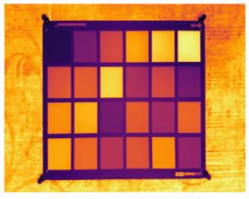 Denoised Image (30.99/0.9276)	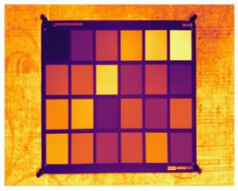 Denoised Image (37.03/0.9822)	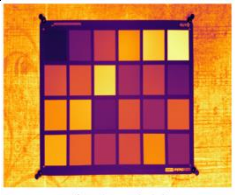 Clean Image (∞/∞)
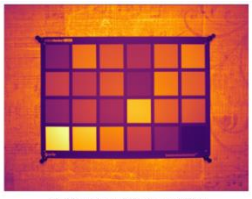 Noisy Image (46.41/0.9946)	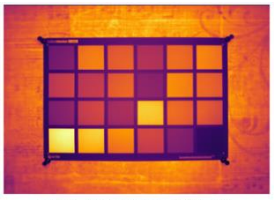 Denoised Image (35.66/0.9352)	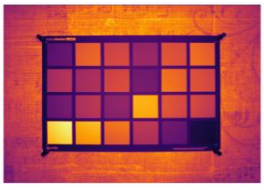 Denoised Image (38.36/0.9846)	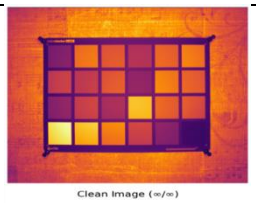 Clean Image (∞/∞)
 Noisy Image (46.25/0.9965)	 Denoised Image (30.51/0.9606)	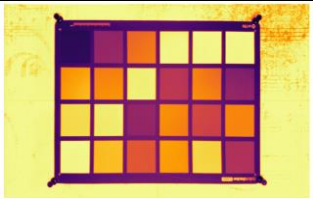 Denoised Image (36.14/0.9816)	 Clean Image (∞/∞)

Table 5. Result of DND Dataset

Noisy Image	HI-GAN Denoised Image	Denoised Image by Our Method	Clean Image
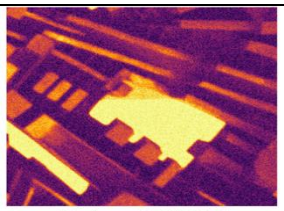 Noisy Image (20.07/0.2798)	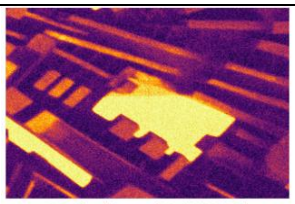 Denoised Image (25.40/0.6006)	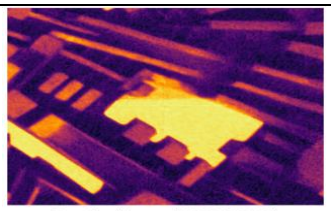 Denoised Image (25.93/0.8073)	 Clean Image (∞/∞)
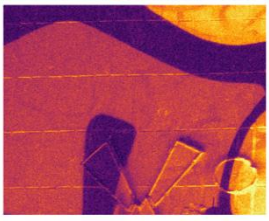 Noisy Image (22.80/0.2862)	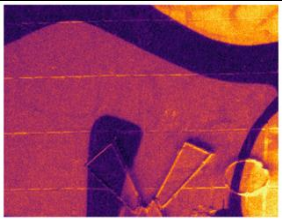 Denoised Image (26.46/0.5714)	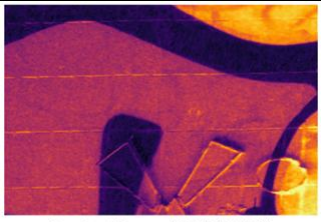 Denoised Image (30.70/0.8384)	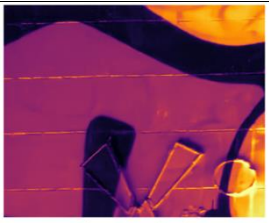 Clean Image (∞/∞)
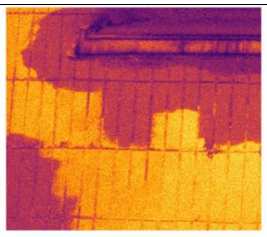 Noisy Image (23.04/0.2934)	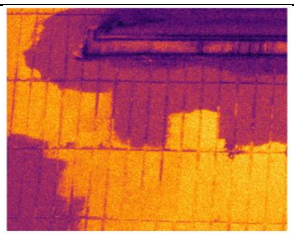 Denoised Image (26.70/0.6029)	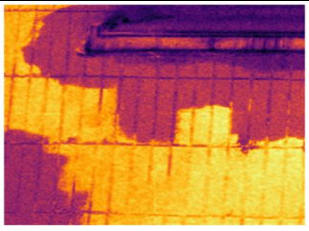 Denoised Image (32.57/0.8685)	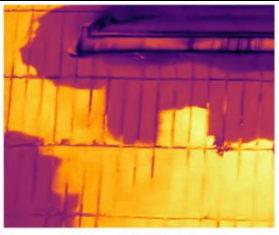 Clean Image (∞/∞)
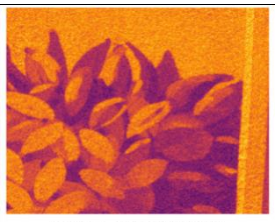 Noisy Image (22.72/0.2744)	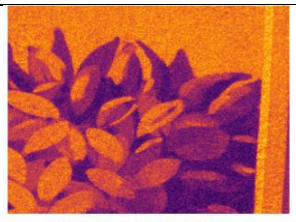 Denoised Image (26.27/0.5861)	 Denoised Image (32.36/0.8437)	 Clean Image (∞/∞)

Table 6. Result of FFHQ Dataset

Noisy Image	HI-GAN Denoised Image	Denoised Image by Our Method	Clean Image
 Noisy Image (24.00/0.3689)	 Denoised Image (27.00/0.6052)	 Denoised Image (32.66/0.9205)	 Clean Image (∞/∞)

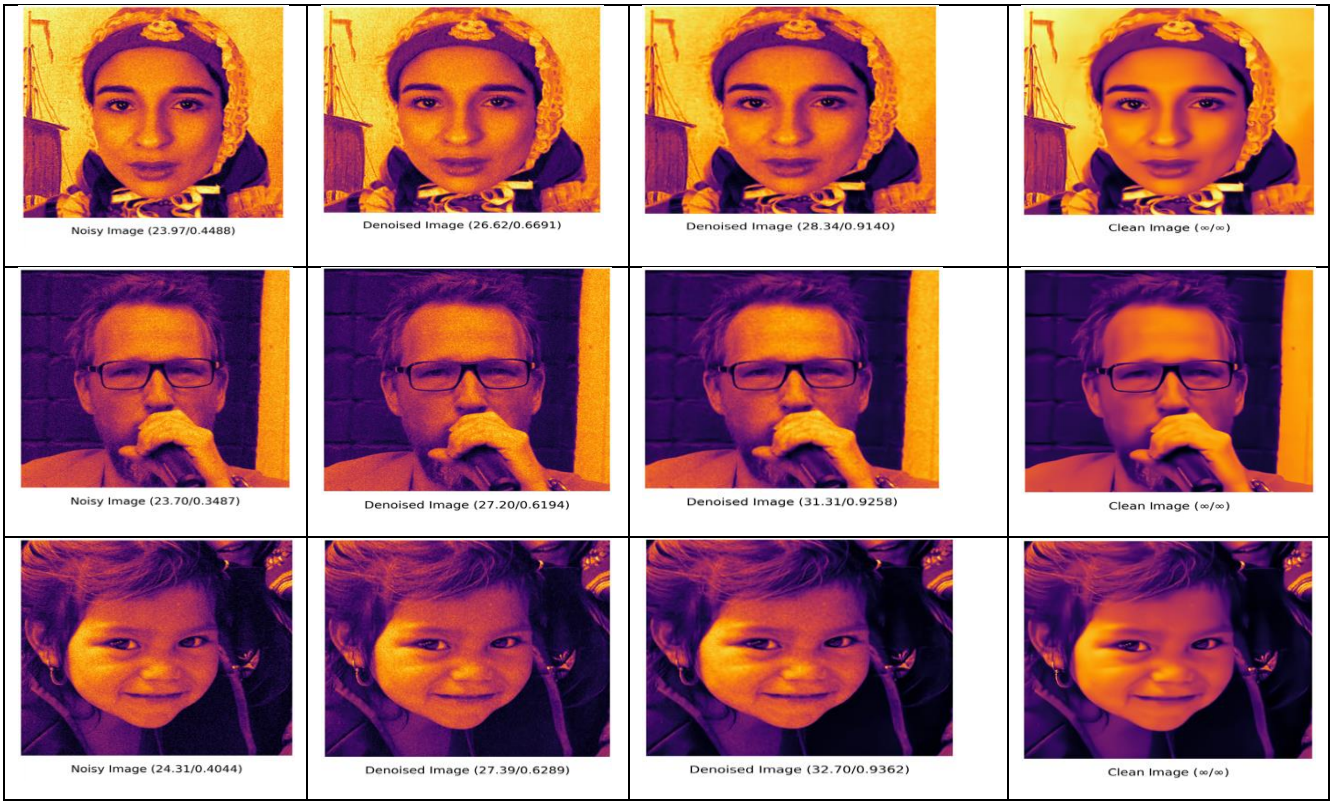

Table 7. Result of NAM Dataset

Noisy Image	HI-GAN Denoised Image	Denoised Image by Our Method	Clean Image
 Noisy Image (35.39/0.9369)	 Denoised Image (34.73/0.9458)	 Denoised Image (36.19/0.9643)	 Clean Image (∞/∞)
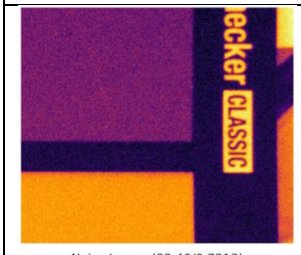 Noisy Image (32.40/0.7213)	 Denoised Image (33.65/0.8406)	 Denoised Image (37.07/0.9516)	 Clean Image (∞/∞)
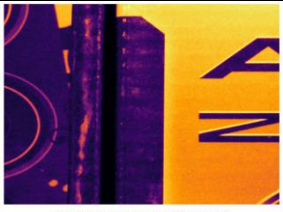 Noisy Image (39.11/0.9339)	 Denoised Image (38.98/0.9529)	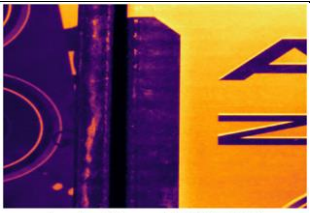 Denoised Image (40.65/0.9732)	 Clean Image (∞/∞)

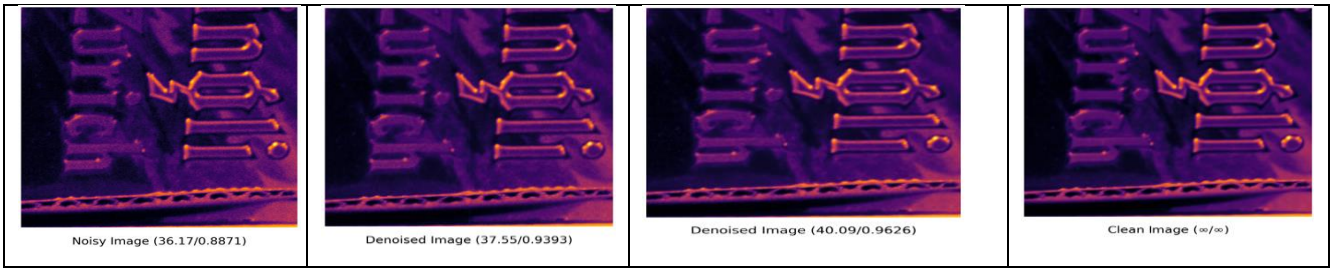

Conclusions

The research proposes an enhanced HIGAN model for picture denoising, which achieves good perceptual quality in terms of both general content and specific features. The trained model performs remarkably well in single frame denoising, and it can maintain key features without losing perceptible details, thanks to the modified loss function. The dense connections between each layer within each RDB allow for full utilization of local features, along with the added parallel skipped network, resulting in an efficient approach to achieving our goal of denoising images without losing any important features. The local feature fusion (LFF) not only stabilizes the training of wider networks, but also adaptively controls the preservation of information from the current and preceding RDBs. RDB also allows for direct connections between the preceding RDB and each layer of the current block, resulting in a contiguous memory (CM) mechanism. Additionally, the local residual learning (LRL) further improves the flow of information and gradients. Since ReLU is computationally efficient as only a certain number of neurons are activated the proposed HIGAN model with the modified Residual Dense Block (RDB) led to an increase in the PSNR and SSIM of images. However, for practical purposes, we frequently have to deal with noisy low-resolution photos. The two picture processing techniques of traditional interpolation and noise reduction may collide. Further investigation into the impact of combined SR and denoising on damaged photos may therefore be highly motivating**.**

Funding: The research did not receive financial assistance from any funding entity.

Conflicts of Interest: The author has no conflicts of interest to disclose concerning this study.

Declarations: This manuscript has not been published to any other journal or online sources.

Data Availability: The author has all the data employed in this research and is open to sharing it upon reasonable request.

REFERENCES

Burger, Harold C., Christian J. Schuler, Stefan Harmeling. "Image denoising: Can plain neural networks compete with BM3D?." IEEE conference on computer vision and pattern recognition. 2012.

Xie, Junyuan, Linli Xu, Enhong Chen. "Image denoising and inpainting with deep neural networks." Advances in neural information processing systems. 2012.

Agostinelli, Forest, Michael R. Anderson, Honglak Lee. "Adaptive multi-column deep neural networks with application to robust image denoising." Advances in neural information processing systems. 2013.

Li, HuiMing. "Deep learning for image denoising." International Journal of Signal Processing, Image Processing and Pattern Recognition. 2014.

Isa, Iza Sazanita. "Evaluating denoising performances of fundamental filters for T2-weighted MRI images." Procedia Computer Science 60. 2015.

Zhang, Xin, Ruiyuan Wu. "Fast depth image denoising and enhacement using a deep convolutional network." IEEE International Conference on Acoustics Speech and Signal Processing(ICASSP). 2016.

S. Nam, Y. Hwang, Y. Matsushita, S. J. Kim. "A holistic approach to cross-channel image modelling and its application to image denoising." IEEE Computer Vision and Pattern Recognition(CVPR). 2016.

Zhang, Kai. "Beyond a gaussian denoiser: Residual learning of deep cnn for image denoising." IEEE transactions on image processing. 2017.

T. Plotz, S. Roth. "Benchmarking denoising algorithms with real photographs." IEEE Computer Vision and Pattern Recognition(CVPR). 2017.

Liu, Zhe, Wei Qi Yan, Mee Loong Yang. "Image denoising based on a CNN model." 4th International Conference on Control Automation and Robotics(ICCAR). 2018.

Sun, Yuewen. "Digital radiography image denoising using a generative adversarial network." Journal of X-ray Science and Technology. 2018.

A.Abdelhamed S. Lin, M. S. Brown. " A high-quality denoising dataset for smart phone cameras." IEEE Computer Vision and Pattern Recognition(CVPR). 2018.

Zhang, Kai, Wangmeng Zuo, and Lei Zhang. "FFDNet: Toward a fast and flexible solution for CNN-based image denoising." IEEE Transactions on Image Processing. 2018.

Yu, Songhyun, Bumjun Park, Jechang Jeong. "Deep iterative down-up cnn image bdenoising." Proceedings of the IEEE/CVF Conference on Computer Vision and Pattern Recognition Workshops. 2019.

Gu, Shuhang, et al. "Self-guided network for fast image denoising." Proceedings of the IEEE/CVF International Conference on Computer Vision. 2019.

Krull, Alexander, Tim-Oliver Buchholz, Florian Jug. "Noise2void-learning denoising from single noisy images." Proceedings of the IEEE/CVF Conference on Computer Vision and Pattern Recognition. 2019.

Fan, Linwei. "Brief review of image denoising techniques." Visual Computing for Industry, Biomedicine, and Art. 2019.

Chunwei Tian, et al. "Image denoising using deep CNN with batch renormalization." Proceedings of the IEEE/CVF Conference on Computer Vision and Pattern Recognition. 2019.

Ghose, Shreyasi, Nishi Singh, Prabhishek Singh. "Image denoising using deep learning: Convolutional neural network." 10th International Conference on Cloud Computing, Data Science & Engineering (Confluence). 2020.

Kumwilaisak, Wuttipong. "Image denoising with deep convolutional neural and multi-directional long short-term memory networks under Poisson noise environments." IEEE Access 8. 2020.

Babu, Dinsha, Sajeev K Jose. "Review on CNN Based Image Denoising." Review on CNN Based Image Denoising. 2020.

Tian, Chunwei. "Deep learning on image denoising: An overview." Neural Networks. 2020.

Wei, Kaixuan. "A physics-based noise formation model for extreme low-light raw denoising." Proceedings of the IEEE/CVF Conference on Computer Vision and Pattern Recognition. 2020.

Peizhu Gong, Jin Liu, Shiqi Lv. "Image Denoising with GAN Based Model." Journal of Information Hiding and Privacy Protection. 2020.

Ilesanmi, Ademola E., Taiwo O. Ilesanmi. "Methods for image denoising using convolutional neural network: a review." Complex & Intelligent Systems. 2021.

Duc My Vo, Duc Manh Nguyen, Thao Phuong Le, Sang-Woong Lee. " HI-GAN: A hierarchical generative

adversarial network for blind denoising of real photographs." Proceedings of the IEEE/CVF Conference on Computer Vision and Pattern Recognition Workshops. 2021.

Alam et al., 2025. (2025a). Online Corrective Feedback and Self-Regulated Writing: Exploring Student Perceptions and Challenges in Higher Education. 15(06), 139–150. https://doi.org/https://doi.org/10.5430/wjel.v15n6p139

Hossen, M. S., Pauzi, H. B. M., & Salleh, S. F. B. (2023). Enhancing Elderly Well-being Through Age-Friendly Community, Social Engagement and Social Support. American J Sci Edu Re: AJSER-135.

Hossen, M. S., Pauzi, H. M., Islam, M. S., & Salleh, S. F. (2026). ELDERLY LIFE SATISFACTION THROUGH SOCIAL INTERACTION AND FORMAL CARE CENTER MANAGEMENT. Asian People Journal (APJ), 9(1), 1–15.

Mohd Pauzi, H., & Shahadat Hossen, M. (2025). Comprehensive bibliometric integration of formal social support literature for elderly individuals. Housing, Care and Support, 1–17.

Rahman, M. K., Hossain, M. A., Ismail, N. A., Hossen, M. S., & Sultana, M. (2025). Determinants of students' adoption of AI chatbots in higher education: the moderating role of tech readiness. Interactive Technology and Smart Education.

Rashed, M., Jamadar, Y., Hossen, M. S., Islam, M. F., Thakur, O. A., & Uddin, M. K. (2025). Sustainability catalysts and green growth: Triangulating evidence from EU countries using panel data, MMQR, and CCEMG. Green Technologies and Sustainability, 100305.